POLISH MARITIME RESEARCH 3 (127) 2025 Vol. 32; pp. 163-170
10.2478/pomr-2025-0044

NUMERICAL SIMULATION TO INVESTIGATE THE INFLUENCE OF WELDING SEQUENCES AND BOUNDARY CONDITIONS ON THE MECHANICAL BEHAVIOUR OF GUSSET JOINTS

Eric Caballero [1]
Hector Ruiz [2, 3, 4 *]
Juan Blandon [1]
[1] School of Mechanical, Technological University of Panama, Panama City, Panama
[2] Research and Innovation Center for Education, Science and Technology (CIIECYT-AIP), Panama City, Panama
[3] Specialized Superior Technical Institute (ITSE), Panama City, Panama
[4] The National Research System (SNI), SENACYT, Panama City, Panama

* Corresponding author: *hruiz@ciiecyt.org.pa (Hector Ruiz)*

ABSTRACT

Welding is one of the most widely used joining processes for the fabrication of steel parts. Consequently, it is commonly used in the shipbuilding industry for the fabrication of structural T-stiffeners. However, this process introduces inherent imperfections, such as angular deformation and residual stresses, which can affect structural stability and shorten the lifespan of the parts. This study conducts a literature review to replicate numerical analyses from reference studies, validating the proposed simulation methodology by comparing numerical and experimental thermo-mechanical results. A finite element model is created using MSC Patran and the welding process is simulated with Simufact Welding. Once the methodology is validated, a case study is conducted in which the shielded metal arc welding (SMAW) process is simulated using a simultaneously coupled thermo-elasto-plastic analysis, based on the finite element method. The study aims to determine the influence of welding sequences and mechanical boundary conditions on angular deformation and longitudinal residual stresses in the T-joints of narrow and thin plates made of S355J2 structural steel. These plates are used as structural stiffeners in the stern and bow sections of patrol boats. The goal is to propose an optimal welding sequence and boundary condition configuration that mitigates angular distortion and longitudinal residual stresses in the structural members. The proposed welding sequence consists of four weld lines running from the middle of the plate to the end, whilst the mechanical boundary condition supports the plate along the longitudinal ends.

Keywords: Angular deformation; Mechanical boundary conditions; Residual stresses; Structural stiffeners; Welding sequences

INTRODUCTION

Welding is a widely used process for joining metal parts in various industries, due to its versatility, flexibility, efficiency, and low cost. However, it induces thermal stresses that generate angular deformations and residual tensile stresses in the structure. These imperfections are consequences of the non-homogeneous thermal cycle, which compromises the structural integrity and service life of welded parts [1], [2].

During the welding process, parts are joined through specific welding sequences. To ensure stability, mechanical boundary conditions are applied beforehand, to restrict movements. These constraints support the parts and prevent unwanted displacement during the application of welding beads [3], [4]. Over recent decades, various researchers have carried out investigations to mitigate welding imperfections through the optimisation of welding sequences and mechanical boundary conditions. Computational analysis has become a powerful tool for investigating welding imperfections due to residual stress and deformation, particularly through the Finite Element Method (FEM) [5], [6]. Fu [3] analysed the influence of welding sequences on angular deformation and residual stresses in a T-joint through numerical simulations and experimental validation. They pointed out the fact that welding sequences significantly influence the magnitude and behaviour of angular deformation. Chen et al. [7] carried out a numerical simulation to analyse the temperature distribution, welding deformation, and residual stresses in T-joints produced by various welding sequences. They concluded that two shorter weld lines result in less deformation, compared to a continuous weld line. As a result, the direction of the welding line significantly impacts the magnitude of angular deformation [8]. Similarly, symmetrical welding sequences generate less deformation than asymmetrical welding sequence [9]. Therefore, welding sequences influence increases in residual stresses but not their behaviour [10]. Nevertheless, most of these studies focused on the Gas Metal Arc Welding (GMAW) process applied to different types of steel joints because it is commonly used for its efficiency, finish and flexibility (i.e. for welding different materials).

Mechanical boundary conditions support the plates during the welding process, limiting the expansion and contraction movements of the plates, and influencing the angular deformation and residual stresses [4]. Fanous et al. [11] investigated the effect of boundary conditions on residual stresses in a flat plate, through numerical simulations using the Finite Element Method (FEM). In that study, it was concluded that variations in boundary conditions have a greater impact on residual stresses, compared to those generated during the welding process. Zhang and Wang [12] analysed the influence of mechanical boundary conditions on the deformation caused by welding and residual stresses in a reinforced panel using FEM, determining that the symmetry of the boundary conditions reduces the magnitude of global and local deformation in the structure, as well as reducing residual stresses. On the other hand, Deng [13] investigated the influence of mechanical constraints on deformation and residual stresses in a butt weld of thin plates, through a Thermo-Elasto-Plastic Analysis (TEPA). They concluded that mechanical constraints can mitigate the magnitude of the final deformation; however, it is not possible to eliminate deformation solely by varying these constraints. Therefore, whilst increasing mechanical constraints can reduce deformation, it can also lead to an increase in residual stresses [14].

Imperfections, such as angular deformation and tensile residual stress, remain a challenge for the industry. Minimising their generation and influence is crucial, as these imperfections can compromise the structural integrity and service life of components [15]. This study focuses on analysing the impact of welding sequences and mechanical boundary conditions on angular deformation and residual stresses in the thin, narrow plate T-joints used as structural stiffeners in patrol boats. The Shielded Metal Arc Welding (SMAW) process is considered to be the method used by technicians in the local shipyard. Numerical simulations were conducted, using a simultaneously coupled TEPA by FEM, in order to propose an optimal combination of sequences and restrictions to mitigate welding imperfections when the SMAW process is employed.

METHODOLOGY

CASE STUDY

In this study, various welding sequences and boundary conditions are proposed, to determine their influence on angular welding deformation and residual stresses in the thin, narrow structural stiffeners used in steel patrol boats. Simultaneously coupled TEPA was employed, using FEM, to investigate the reliability of the simulations. Two reference cases were compared: an experimental case [16] and a simulation case [10].

REVIEW AND COMPARISON WITH REFERENCES

Review of the experimental studies

Deng's study [16] determined the angular deformation of a T-joint made of thin S235 steel plates (SM400A) through numerical analysis and experimental testing. The study considered rigid body motion (RBM) as a boundary condition and a leg length of 6 mm (as shown in Fig. 1) A fine mesh was considered in the Heat-Affected Zone (HAZ), with dimensions of 2.25 x 3.00 x 5.00 mm. The welding conditions used by Deng were 290 A, 29 V, and 6.67 mm/s, with an efficiency of 80%. The commercial finite element software 'Abaqus' was utilised for the numerical analysis. Simulations were conducted using an uncoupled TEPA, to calculate the angular deformations measured at three lines, including the mid-section of the joint. A Gaussian distribution was used as the mathematical model for the heat source. In the experiments, a robot was used to perform welding lines using the GMAW process; angular deformation was measured on the upper surface of the horizontal plate after welding, as shown in Fig. 6.

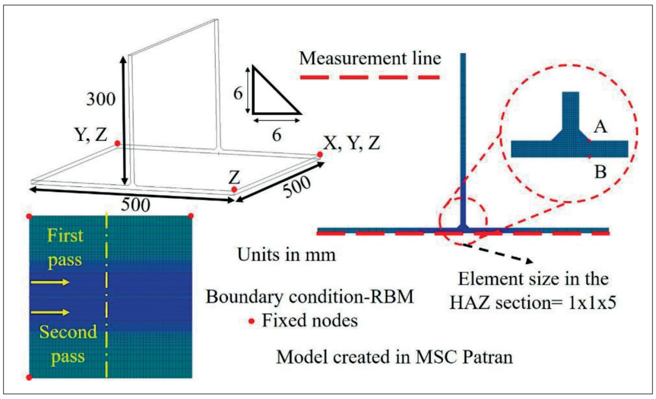

Fig. 1. Finite element model and dimensions created in MSC Patran

Review of the numerical study

Gannon's study [10] evaluated the angular deformation caused by welding sequences in a T-joint of thin plates of S235 (SM400A) through numerical simulations. Rigid body motion (RBM) was considered as a boundary condition, fixing three corners of the base plate on the lower surface, as illustrated in Fig. 1, and considering fine mesh in the HAZ, with dimensions of 0.50 x 0.75 x 10.00 mm. The study validated the methodology by comparing it with the experimental results of angular deformation reported by Deng [16], using the same process and welding conditions. Using the commercial software 'ANSYS', Gannon performed a sequentially coupled TEPA. The mathematical model for the heat source was a Gaussian distribution. The angular deformation results were measured at the mid-section of the flange plate on the lower surface. Therefore, based on the methodologies of both studies, the numerical, thermal and mechanical results reported by Gannon were compared [10]. Comparison between the numerical results of Gannon and the experimental results reported by Deng showed a difference in the angular deformation of approximately 5.5%. This comparison can be observed in Fig. 6.

NUMERICAL ANALYSIS

To analyse the influence of welding sequences and mechanical boundary conditions, TEPA coupling was employed. This involved thermal analysis, to evaluate the temperature distribution, simultaneous with mechanical analysis, to calculate the angular deformations and residual stresses induced by the thermal load[17].

The governing equation for the thermal analysis is Fourier´s law, Eq. (1), expressed in Cartesian coordinates, where 'T' is temperature (measured in °C), coordinates are in mm (x, y, z) and 'Q' is heat input, in units of J/mm. The thermal conductivity (k-W/mm °C) and heat capacity (ρC-J/mm^3 °C) are temperature-dependent properties, which introduce non-linearity into the analysis [18].

$$\frac{\partial}{\partial x}\left[\left(k(T)\right)\frac{\partial T}{\partial x}\right]+\frac{\partial}{\partial y}\left[\left(k(T)\right)\frac{\partial T}{\partial y}\right]+\frac{\partial}{\partial x}\left[\left(k(T)\right)\frac{\partial T}{\partial z}\right] = \rho C(T)\,\frac{\partial T}{\partial t}-Q \quad (1)$$

On the other hand, the equation governing the mechanical analysis is the force-displacement relationship, based on Hooke´s law for non-linear analyses, Eq. (2), where the stiffness matrix (K) is dependent on both the material properties and the deformed geometry. Force is determined by 'P' and 'u' is displacement [19].

$$P = K\,(P, u)\;u \quad (2)$$

These equations are integrated into the commercial software MSC Marc [20], which is the solver for the commercial simulation software 'Simufact welding' [21].

MODEL FOR COMPARISON WITH REFERENCES

The finite element model shown in Fig. 1 was used to validate the proposed methodology by replicating the numerical analysis carried out by [10]. The numerical results were then compared with the experimental results of angular deformation reported by [16]. For this simulation, the same welding conditions and boundary conditions used in the reference studies were considered, where the element type and the mathematical model of the heat source varied, using the commercial software 'Simufact welding' [21].

MESH SENSITIVITY ANALYSES

To determine the optimal mesh size in the HAZ, a sensitivity analysis was carried out; two differences models were evaluated using the joint dimensions in Fig. 1. In the models, the height and width of the element in the HAZ is 1 mm for both dimensions, varying the length of the element (see Table 1). We considered the maximum aspect ratio of 1:10 mm, which was recommended by Simufact Welding, for the simulation of welding processes, and considered the mesh length used by [10], [16].

Tab. 1. Length of element in the HAZ

Models	M1	M2	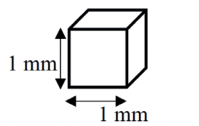
Length of element (mm)	5	10	

Finite element model for case study

The finite element model for this study was created using the commercial software 'MSC Patran' [22], as shown in Fig. 2. Hexahedral elements were used, with a fine mesh in the Heat-Affected Zone (HAZ), to achieve greater accuracy in the thermal results. The dimensions of the T-joint were obtained from the structural stiffeners of a patrol boat. The material considered for this study was S355J2 low-carbon steel, which is used in a local shipyard for the corrective maintenance of one of the boats. The thermal-mechanical properties were obtained from the Simufact Material software database [21]. Despite considering the phase transformation of the material on welding processes, it showed a significant influence on the welding corrosion resistance [23]. This study did not consider phase transformation of the material because it has no significant influence on the angular welding deformation and residual stresses [24].

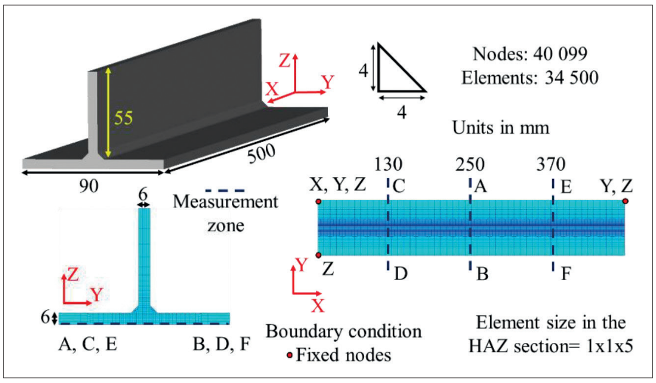

Fig. 2. Finite element model of the case studies

The SMAW welding process was considered, with welding conditions obtained in the field (see Table 2). The mathematical model of the heat source used in the simulation program was the Goldak double ellipsoid [25] with the dimensions: front length (af) 1.5 mm, rear length (ar) 3.0 mm, depth (d) 4.0 mm, and half of breadth (b) 4.0 mm. The heat input produced by the welding conditions was calculated using Eq. (3), showing a 92% similarity to that used in the study by [7], which applied a GMAW process to a 6 mm thick T-joint. The parameters considered in the welding conditions were verified in the field with a plate thickness of 6 mm because those parameters are important for the prediction of welding deformation [26].

Tab. 2. Welding condition

Amperage (A)	Voltage (V)	Welding speed, ν (mm/s)	Efficiency, η	Heat input (J/mm)
90	23.6	2.2	0.8	772.36

$$Q = \frac{AV\eta}{v} \quad (3)$$

Welding sequence analyses

The effect of welding sequences on angular deformation and residual stresses was evaluated through numerical simulation (see Fig. 3). Sequences A, B, and C were based on those used in the studies by [3] and [27]. Additionally, sequences D, E, and F were proposed by the authors, based on sequences used by technicians at the shipyard. In this stage, the mechanical constraint used was the rigid body motion (RBM) condition, which is an idealised condition commonly used in numerical analyses [28], [29]. The angular deformation and residual stresses were evaluated in the cross-section on the lower surface of the flange plate, along lines A-B, C-D and E-F, as shown in Fig. 2.

Mechanical boundary condition analysis

The evaluation of mechanical boundary conditions was carried out after selecting a welding sequence that exhibited uniform and lower magnitude angular welding deformation and residual stresses. Different mechanical constraint configurations were proposed, as shown in Fig. 3.

- The BC-A condition is the idealised boundary condition, where the six degrees of freedom are restricted by fixing three nodes located at the corners of the flange plate.
- The BC-B condition, commonly referred to as the 'table' condition, is frequently observed in shipyards. Additionally, two corners are fixed using clamps on the upper surface of the flange plate. The clamps on the lower left-hand corner are fixed during the first and second passes. Afterwards, they are removed, and the clamps on the upper right-hand corner are activated until the welding lines are completed.
- BC-C is a proposed condition where the plate rests on all four corners, with two of the corners fixed on the upper surface, similar to the fixation in the BC-B condition.
- In BC-D, the four corners are fixed. They are separated into two conditions: BC-D1 consists of keeping the upper constraints fixed during the welding process until the cooling stage; whereas, in the BC-D2 condition, the upper constraints are removed during the final cooling stage [4].
- The other proposed boundary conditions are variations of the table condition, considering transverse supports (BC-E) and longitudinal supports (BC-F). The corners are fixed with upper clamps, similar to the procedure used in condition BC-B.

RESULTS AND DISCUSSION

COMPARISON BETWEEN CASE STUDIES AND MESH SENSITIVITY ANALYSIS

Thermal results

The thermal history was assessed at points A and B. At point A, the simulations of the M1 and M2 model of this study yield maximum temperatures of 1624°C and 1433°C, respectively, while Gannon [10] reported 1730°C. At point B, the simulation gives 485°C for the M1 model, while M2 gives a temperature of 460°C, compared to Gannon's 500°C. Thus, the temperature difference is approximately 6% at point A and 2% at point B for the M1 model. For M2, no heat penetration is obtained, reaching a difference of 17%, as shown in Fig. 4. The difference may result from factors such as the use of different numerical analysis software, variations in the mesh, differences in the material's thermo-mechanical properties (as they were sourced from different databases), and discrepancies in the mathematical heat source model and dimensions.

Mechanical results

In the mechanical results, the angular deformation obtained by Gannon [10] was 3.04°, while the simulated maximum

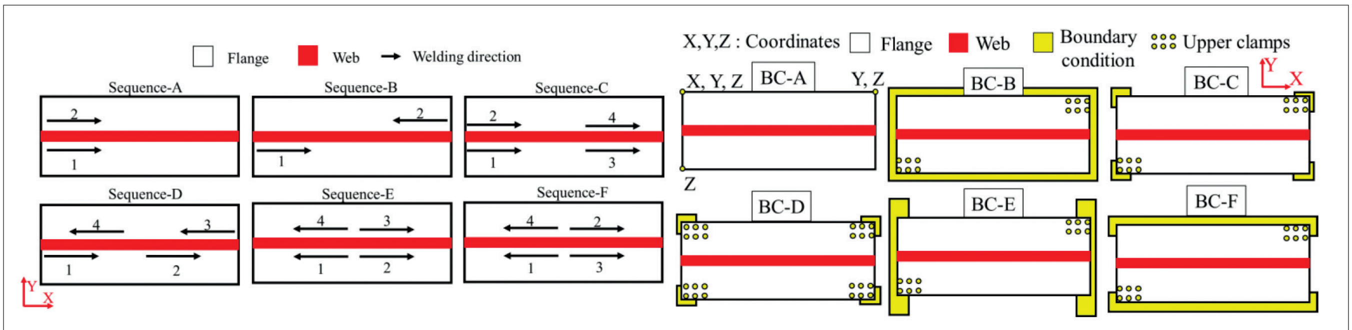

Fig. 3. Welding sequence and mechanical boundary conditions

deformation reaches 3.00°, yielding a difference of approximately 2%, as shown in Fig. 4. In turn, the simulated results were compared with the experimental results of [16] showing a difference of approximately 5%. The difference between the M2 model and Gannon´s results was also approximately 5%; however, as it did not achieve a good penetration, it is neglected.

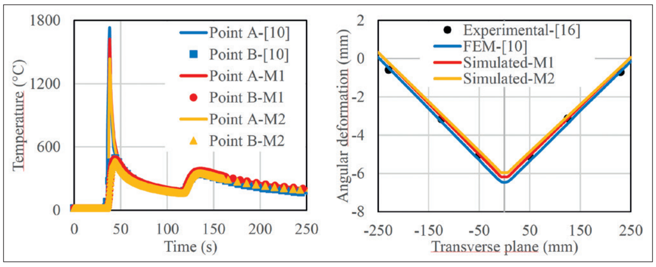

Fig. 4. Thermal history and angular deformation comparison

This difference may stem from variations in the thermal results, mechanical properties, and mesh size. However, the similarity in thermo-mechanical results suggests that the proposed methodology is effective for analysing welding sequences and boundary conditions.

WELDING SEQUENCE ANALYSIS

Thermal results

The thermal results are shown in Fig. 5, where the weld pool from the welding sequences is observed, along with the thermal history measured in the constant section of the weld bead. The temperature reached is similar to the 1600°C reported by [7]. With constant welding conditions, the weld pool and thermal history across the different welding sequences remain similar, with negligible differences.

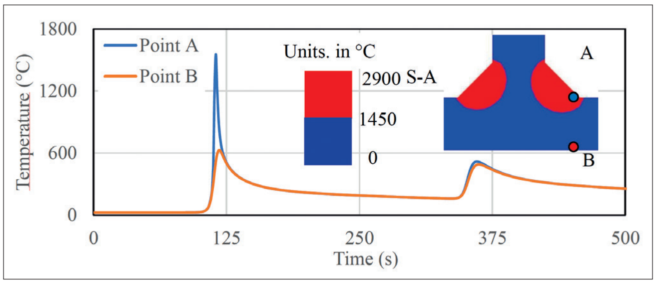

Fig. 5. Weld pool and thermal history

Mechanical results

Simulations of the welding sequences reveal that they influence the behaviour and magnitude of angular deformation, as noted by [3]. Fig. 6 shows the angular deformation caused by the different sequences, measured along lines A-B. Sequences E and F exhibit uniform behaviour, with average deformation angles of 3.28° and 3.29°, respectively, compared to sequence A (3.54°), resulting in an approximate difference of 7% (see Table 3). This may be due to the more uniform heat distribution in sequences E and F, which allows better control over the angular deformation.

On the other hand, the residual stresses from the different welding sequences (Fig. 7) show no significant difference along lines C-D and E-F. However, in the middle of the plate (A-B), a discontinuous zone occurs due to the start and end of the welding lines in sequences C, D, E, and F, where atypical behaviour is observed. Therefore, residual stresses are not considered in this section. The similarity of residual stresses in the stable zone of the welding lines (C-D; E-F) is due to the fact that the heat input does not affect the behaviour or magnitude.

Consequently, sequence E was selected for the analysis of boundary conditions, due to its low perpendicular displacement, uniform and lower magnitude of angular deformation, and residual stresses which were consistent with those obtained by [3].

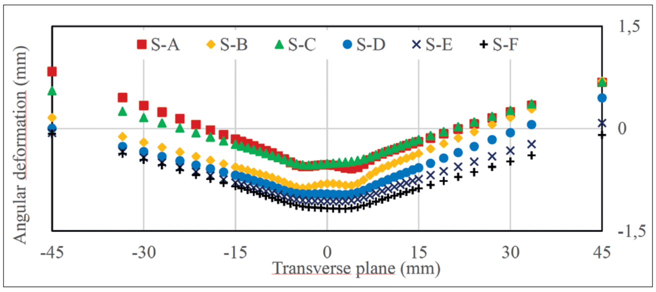

Fig. 6. Angular deformation caused by welding sequences

Tab. 3. Deformation angle and their differences

Lines	S-A	S-B	S-C	S-D	S-E	S-F
C-D	3.45°	3.45°	3.33°	3.45°	3.55°	3.53°
A-B	3.56°	3.41°	3.15°	3.30°	3.00°	3.02°
E-F	3.60°	3.25°	3.43°	3.20°	3.30°	3.30°
Avg.	3.54°	3.37°	3.30°	3.32°	3.28°	3.29°
Diff. %		-4.78	-6.67	-6.25	-7.19	-7.14

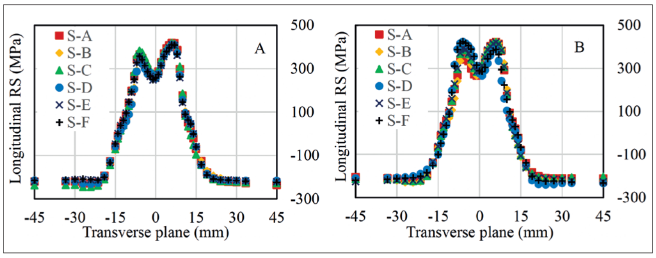

Fig. 7. Longitudinal residual stresses (RS). A) measured in C-D, B) measured in E-F

MECHANICAL BOUNDARY CONDITIONS ANALYSIS

The mechanical results from simulations with different boundary conditions show that angular deformation (Fig. 8) varies based on the constraint configuration. This is because the supports limit the joint's expansion and contraction movements. Table 4 presents the differences between the boundary conditions compared to the BC-B condition.

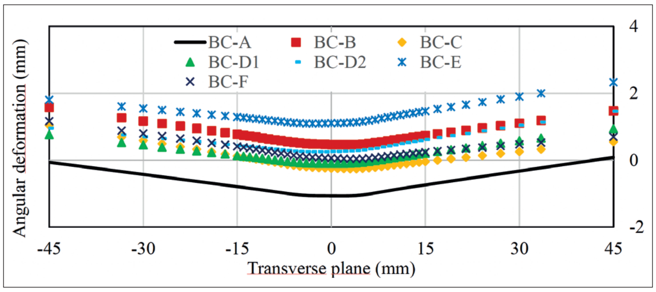

Fig. 8. Angular deformation caused by boundary conditions

The residual stresses measured along lines C-D and E-F are shown in Fig. 9. Line A-B represents a discontinuity zone. However, in the stable section of the welding line, the boundary conditions do not significantly affect the magnitude or behaviour of the residual stresses, except for the BC-D1 condition. In BC-D1, the joint is restricted during and after the welding sequence, resulting in residual longitudinal tensile stresses in both measurement lines. In contrast, the BC-D2 condition, despite similarities, involves releasing the upper clamps once the weld line application is completed. This behaviour aligns with the findings of [14].

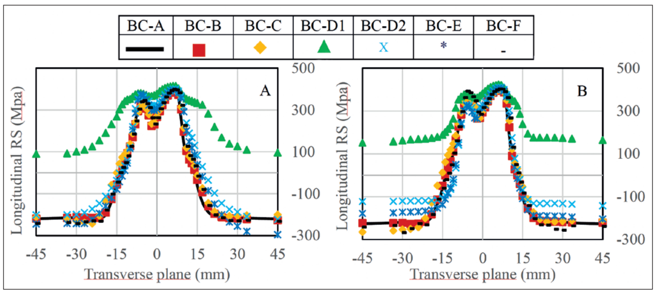

Fig. 9. Longitudinal residual stresses (RS) A) Measured in C-D, B) Measured in E-F

Furthermore, the BC-F condition, which restricts the end of the longitudinal section with the upper clamps, shows uniform behaviour with a low magnitude of perpendicular displacement. This is because it does not over-constrain the joint during the welding process, unlike the BC-D1 condition. While BC-D1 reduces angular deformation by 12%, compared to BC-B, it limits the joint's expansion and contraction, leading to an increase in residual longitudinal tensile stresses.

Tab. 4. Deformation angle and their differences

Lines	BC-A	BC-B	BC-C	BC-D1	BC-D2	BC-E	BC-F
C-D	3.55°	3.53°	3.48°	3.17°	3.23°	3.29°	2.88°
A-B	3.00°	2.97°	2.92°	2.64°	2.65°	2.67°	2.41°
E-F	3.30°	3.32°	3.26°	2.96°	3.00°	3.07°	2.54°
Avg.	3.28°	3.27°	3.22°	2.91°	2.96°	3.01°	2.61°
Diff. %	–	-0.27	-1.86	-12.28	-10.90	-9.11	-25.72

In order to propose an optimal combination of welding sequence and boundary conditions, sequences A and E were evaluated using the BC-F boundary condition. Fig. 10 shows the angular deformation caused by sequences A and E, measured in the zones at 130, 250, and 370 mm (C-D, A-B, E-F), while residual stresses are evaluated in the C-D and E-F zones, as shown in Fig. 2. In the middle of the plate (A-B), sequence A results in a deformation angle of 2.95°, with non-uniform behaviour being observed, as the left flange experiences a greater deformation angle than the right flange. Sequence E, on the other hand, results in a deformation angle of 2.41°, representing a difference of approximately 23%. The residual longitudinal stress results show a negligible difference.

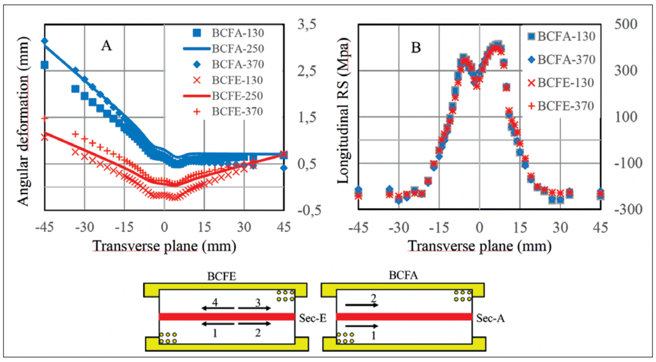

Fig. 10. Comparison of sequences A and E. A) Angular deformation, B) Longitudinal residual stresses

CONCLUSIONS

This study determined the influence of welding sequences and boundary conditions on imperfections, such as angular deformation and residual stresses in T-joints, through numerical simulations.

WELDING SEQUENCE

- The welding sequence influences the behaviour and magnitude of angular deformation because heat is applied along the weld lines. If the heat is induced non-uniformly, it affects both the behaviour and magnitude of the angular deformation.
- Sequences that involve a weld bead from end to end, such as sequences A and B, induce heat unevenly, resulting in deformation angles of 3.54° and 3.37°, respectively. These are the largest angles observed among the sequences considered.
- Sequences E and F, where welding lines are applied from the centre to the ends of the plate, using four beads, induce heat uniformly. This approach allows the joint to dissipate heat during the process, minimising angular deformation by 16%, compared to sequences A and B.
- The residual stresses obtained under the given conditions and welding sequences, as well as the plate dimensions considered in this study, show no significant change in behaviour or magnitude.

MECHANICAL BOUNDARY CONDITION

- The mechanical boundary conditions proposed in this study significantly influence angular deformation and residual stresses, as the type of supports considered affects the results. Supports that allow the natural movement of the structure result in less angular deformation.

- The BC-D1 condition ("Support and clamps at all four corners"), which restricts the base plate during and after the welding process, shows a 12% decrease in the deformation angle compared to the ideal conditions (BC-A) and the BC-B condition. However, due to over-restriction, residual tensile stresses are increased, similar to the findings reported by [14].
- The BC-F condition ("longitudinal restriction and clamps") results in a 20% decrease in angular deformation compared to the BC-B condition, as it allows expansion during the heating cycle and contraction during the cooling cycle.

LIMITATIONS AND RECOMMENDATIONS

- This study is solely based on a numerical analysis, where the methodology and finite element model were calibrated by comparison with other studies; therefore, it is recommended that the numerical results are validated by experimental tests.
- For future work, it is recommended that the influence of welding sequence and boundary conditions is analysed, considering other materials and other welding processes, which are commonly used in shipyards.
- The influence of variations in welding speed has not been considered in this study. However, it is recommended for future works.

ACKNOWLEDGEMENTS

The National Secretariat of Science, Technology and Innovation (SENACYT) is gratefully acknowledged for its financial support, provided through the 2023 public call for new researchers and innovators under code APY-NI-2023A-50.

REFERENCES

1. Ueda Y, Murakawa H, Ma N. Welding Deformation and Residual Stress Prevention, Vol. 1. Elsevier; 2012. doi: https://doi.org/10.1016/B978-0-12-394804-5.00001-3.

2. American Welding Society, Welding manual, 8th ed., Vol. 2. Prentice Hall; 1996.

3. Fu G, Lourenço MI, Duan M, Estefen SF. Influence of the welding sequence on residual stress and distortion of fillet welded structures. Marine Structures, Vol. 46, 2016, pp. 30–55. doi: https://doi.org/10.1016/j.marstruc.2015.12.001.

4. Fu G, Lourenco MI, Duan M, Estefen SF. Effect of boundary conditions on residual stress and distortion in T-joint welds. J Constr Steel Res., Vol. 102, 2014, pp. 121–135. doi: https://doi.org/10.1016/j.jcsr.2014.07.008.

5. Kik T. Computational techniques in numerical simulations of arc and laser welding processes. Materials, Vol. 13, no. 3, Feb. 2020. doi: https://doi.org/10.3390/ma13030608.

6. Das Banik S, Kumar S, Singh PK, Bhattacharya S, Mahapatra mm. Distortion and residual stresses in thick plate weld joint of austenitic stainless steel: Experiments and analysis. J Mater Process Technol, Vol. 289, Mar. 2021. doi: https://doi.org/10.1016/j.jmatprotec.2020.116944.

7. Chen BQ, Guedes Soares C. Effect of welding sequence on temperature distribution, distortions, and residual stress on stiffened plates. International Journal of Advanced Manufacturing Technology, Vol. 86, no. 9–12, 2016, pp. 3145–3156. doi: https://doi.org/10.1007/s00170-016-8448-0.

8. Bai R, Guo Z, Tian C, Lei Z, Yan C, Tao W. Study on welding sequence of butt-welded structures based on equivalent heat source parameter. International Journal of Pressure Vessels and Piping, Vol. 163, 2018, pp. 15–22. doi: https://doi.org/10.1016/j.ijpvp.2018.04.001.

9. Jafarpur K, Nami MR. Analysis of welding conditions based on induced thermal irreversibilities in welded structures: Cases of welding sequences and preheating treatment. Scientia Iranica, Vol. 18, no. 3, 2011, pp. 398–406. doi: https://doi.org/10.1016/j.scient.2011.05.030.

10. Gannon L, Liu Y, Pegg N, Smith M. Effect of welding sequence on residual stress and distortion in flat-bar stiffened plates. Marine Structures, Vol. 23, no. 3, 2010, pp. 385–404. doi: https://doi.org/10.1016/j.marstruc.2010.05.002.

11. Fanous IFZ, Younan MYA, Wifi AS. Study of the Effect of Boundary Conditions on Residual Stresses in Welding Using Element Birth and Element Movement Techniques. Journal of Pressure Vessel Technology, Transactions of the ASME, Vol. 125, no. 4, Nov. 2003, pp. 432–439. doi: https://doi.org/10.1115/1.1613952.

12. Zhang Y, Wang Y. The influence of welding mechanical boundary condition on the residual stress and distortion of a stiffened-panel. Marine Structures, Vol. 65, May 2019, pp. 259–270. doi: https://doi.org/10.1016/j.marstruc.2019.02.007.

13. Deng D, Liu X, He J, Liang W. Investigating the influence of external restraint on welding distortion in thin-plate bead-on joint by means of numerical simulation and experiment. International Journal of Advanced Manufacturing Technology, Vol. 82, no. 5–8, Feb. 2016, pp. 1049–1062. doi: https://doi.org/10.1007/s00170-015-7413-7.

14. Aalami-Aleagha ME, Eslampanah AH. Mechanical constraint effect on residual stress and distortion in T-fillet welds by three-dimensional finite element analysis. Proc Inst Mech Eng B J Eng Manuf., Vol. 227, no. 2, Feb. 2013, pp. 315–323. doi: https://doi.org/10.1177/0954405412466781.

15. Kozak J. Prediction of Weld Deformations by Numerical Methods-Review. Polish Maritime Research, Vol. 29, no. 1, Mar. 2022, pp. 97–107. doi: https://doi.org/10.2478/pomr-2022-0010.

16. Deng D, Liang W, Murakawa H. Determination of welding deformation in fillet-welded joint by means of numerical simulation and comparison with experimental measurements. J Mater Process Technol, Vol. 183, no. 2–3, Mar. 2007, pp. 219–225. doi: https://doi.org/10.1016/j.jmatprotec.2006.10.013.

17. Blandon J, Takaba S, Omae T, Osawa N, Murakawa H. Optimisation of Forming Process of a U-rib by Gas Heating Based on Theoretical Prediction. CMES, Vol. 106, no. 1, 2015, pp. 53–75. doi: https://doi.org/10.3970/cmes.2015.106.053.

18. Pacheco JL, Olmos M. Modelling of Thermal Cycling During Electric Arc Welding of Dissimilar Joints of Stainless Steels Using a Theoretical-Experimental Approach. Revista de la Facultad de Ingeniería, Vol. 30, no. 3, Jul. 2015, pp. 111–118. [Online]. Available: http://ve.scielo.org/scielo.php?script=sci_arttext&pid=S0798-40652015000300011&lng=es&nrm=iso.

19. Hughes TJR. Formulation of Two and Three-Dimensional Boundary Value Problems. In: The finite element method: linear static and dynamic finite element analysis. Courier Corporation, Ed., Courier Corporation, ch. 2; 2003, pp. 57–107.

20. Hexagon AB. Marc Theory and user information. 2023, Hexagon AB.

21. Hexagon AB. Simufact Welding reference manual. 2024, Hexagon AB.

22. Hexagon AB. MSC Patran Reference Manual. 2024, Hexagon AB.

23. Li H, Liu S, Ma Q, Wang P, Liu D, Zhu Q. Investigation of Process Stability and Weld Quality of Underwater Wet Flux-Cored Arc Welding of Low-Alloy High-Strength Steel with Oxy-Rutile Wire. Polish Maritime Research, Vol. 28, no. 3, Sep. 2021, pp. 100–109. doi: https://doi.org/10.2478/pomr-2021-0037.

24. Deng D. FEM prediction of welding residual stress and distortion in carbon steel considering phase transformation effects. Mater Des., Vol. 30, no. 2, Feb. 2009; pp. 359–366. doi: https://doi.org/10.1016/j.matdes.2008.04.052.

25. Goldak J, Chakravarti A, Bibby M. A New Finite Element Model for Welding Heat Sources. Metallurgical Transactions, Vol. 15, no. B, Jun. 1984, pp. 299–305. doi: https://doi.org/10.1007/BF02667333.

26. Urbański T, Banaszek A, Jurczak W. Prediction of Welding-Induced Distortion of Fixed Plate Edge Using Design of Experiment Approach. Polish Maritime Research, Vol. 27, no. 1, Mar. 2020, pp. 134–142. doi: https://doi.org/10.2478/pomr-2020-0014.

27. Bureau Veritas. Rules for the Classification of Steel Ships: Part B Hull and Stability. 2022. [Online]. Available: https://marine-offshore.bureauveritas.com/.

28. Li Z, Feng G, Deng D, Luo Y. Investigating Welding Distortion of Thin-Plate Stiffened Panel Steel Structures by Means of Thermal Elastic Plastic Finite Element Method. J Mater Eng Perform., Vol. 30, no. 5, May 2021, pp. 3677–3690. doi: https://doi.org/10.1007/s11665-021-05646-y.

29. Perić M, Nižetić S, Garašić I, Gubeljak N, Vuherer T, Tonković Z. Numerical calculation and experimental measurement of temperatures and welding residual stresses in a thick-walled T-joint structure. J Therm Anal Calorim., Vol. 141, no. 1, Jan. 2020, pp. 313–322. doi: https://doi.org/10.1007/s10973-019-09231-3.